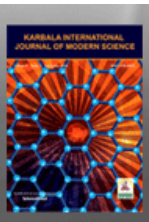

Karbala International Journal of Modern Science

Volume 12 | Issue 2 Article 2

Polyherbal Phytochemicals as Multi-Target Inhibitors of Key Breast Cancer Proteins: A Computational Approach

Nadia Wahyuningsih
Doctoral Program of Biology, Department of Biology, Faculty of Mathematics and Natural Science, Universitas Brawijaya, Malang, Indonesia;

Nashi Widodo
Department of Biology, Faculty of Mathematics and Natural Science, Universitas Brawijaya, Malang, Indonesia.

Sri Rahayu
Department of Biology, Faculty of Mathematics and Natural Science, Universitas Brawijaya, Malang, Indonesia

Muhaimin Rifa'i
Department of Biology, Faculty of Mathematics and Natural Science, Universitas Brawijaya, Malang, Indonesia., rifa123@ub.ac.id

Recommended Citation

Wahyuningsih, Nadia; Widodo, Nashi; Rahayu, Sri; and Rifa'i, Muhaimin (2026) "Polyherbal Phytochemicals as Multi-Target Inhibitors of Key Breast Cancer Proteins: A Computational Approach," *Karbala International Journal of Modern Science*: Vol. 12 : Iss. 2 , Article 2.
Available at: https://doi.org/10.33640/2405-609X.3454

Polyherbal Phytochemicals as Multi-Target Inhibitors of Key Breast Cancer Proteins: A Computational Approach

Abstract

Breast cancer is a primary worldwide health concern, and conventional therapies often cause side effects. This study was performed to investigate the therapeutic potential of a polyherbal formulation containing *Curcuma longa, Phyllanthus niruri, Ziziphus mauritiana, Nigella sativa,* and *Annona muricata* as multi-target inhibitors against breast cancer protein targets using molecular docking and molecular dynamics *in silico* approach. Bioactive compounds were analyzed using Liquid Chromatography High-Resolution Mass Spectrometry (LC-HRMS) to identify the extract's phytochemicals. The compounds were examined for drug-likeness, membrane permeability, bioactivity, and toxicity. The inhibitory ability against the proto-oncogene pathway, which is commonly dysregulated and mutated in breast cancer, including the EGFR and MTOR pathways, was then assessed using molecular docking and dynamics simulations. The findings indicate that various phytochemicals present in the polyherbal formulations demonstrate strong binding affinities and advantageous pharmacokinetic characteristics against MTOR, PIK3CA, and EGFR. This implies their potential as effective multi-target inhibitors. The capability of these bioactive compounds to modulate multiple targets presents a significant advantage compared to therapies that focus on a single target. This study proposes a novel, potent, and non-toxic therapeutic approach for breast cancer

Keywords

Breast cancer, MTOR, PIK3CA, polyherbal medicine, virtual screening

Cover Page Footnote

This research was funded by the Ministry of Higher Education, Science, and Technology of Indonesia in the Program Magister Menuju Doktor untuk Sarjana Unggul (PMDSU) [grant no. 064/C3/ DT.05.00/PL/ 2025].

RESEARCH PAPER

Polyherbal Phytochemicals as Multi-target Inhibitors of Key Breast Cancer Proteins: A Computational Approach

Nadia Wahyuningsih [a], Nashi Widodo [b], Sri Rahayu [b], Muhaimin Rifa'i [b,*]

[a] Doctoral Program of Biology, Department of Biology, Faculty of Mathematics and Natural Science, Universitas Brawijaya, Malang, Indonesia
[b] Department of Biology, Faculty of Mathematics and Natural Science, Universitas Brawijaya, Malang, Indonesia

Abstract

Breast cancer is a primary worldwide health concern, and conventional therapies often cause side effects. This study was performed to investigate the therapeutic potential of a polyherbal formulation containing *Curcuma longa, Phyllanthus niruri, Ziziphus mauritiana, Nigella sativa,* and *Annona muricata* as multi-target inhibitors against breast cancer protein targets using molecular docking and molecular dynamics *in silico* approach. Bioactive compounds were analyzed using Liquid Chromatography High-Resolution Mass Spectrometry (LC-HRMS) to identify the extract's phytochemicals. The compounds were examined for drug-likeness, membrane permeability, bioactivity, and toxicity. The inhibitory ability against the proto-oncogene pathway, which is commonly dysregulated and mutated in breast cancer, including the EGFR and MTOR pathways, was then assessed using molecular docking and dynamics simulations. The findings indicate that various phytochemicals present in the polyherbal formulations demonstrate strong binding affinities and advantageous pharmacokinetic characteristics against MTOR, PIK3CA, and EGFR. This implies their potential as effective multi-target inhibitors. The capability of these bioactive compounds to modulate multiple targets presents a significant advantage compared to therapies that focus on a single target. This study proposes a novel, potent, and non-toxic therapeutic approach for breast cancer.

Keywords: Breast cancer, MTOR, PIK3CA, Polyherbal medicine, Virtual screening

1. Introduction

Breast cancer is a group of different cancers that appear in the mammary glands [1]. Breast cancer caused 670,000 deaths and 2.3 million new cases among women worldwide. The annual rates rose by 1−5% in half of the countries examined [2]. In Indonesia, breast cancer is the most prevalent cancer, with 19.2% of all cancers [3]. There are several common treatments for breast cancer, including chemotherapy, radiotherapy, and surgery, but these treatments cause harmful side effects to the body if used long-term. Fatigue, sleeplessness, peripheral neuropathy, cognitive decline, estrogen deficiency, cardiotoxicity, and secondary malignancies are among the most frequent long-term side effects of chemotherapy [4]. This has encouraged the development of alternative treatments that combine herbal plants as a therapy for breast cancer, known as polyherbal formulations. Polyherbal formulation enhances the synergistic effect to increase the activity of combined substances over the additive effect in a polyherbal combination. This synergistic effect can enhance the antioxidant activity by combining several potent herbal plants [5]. Polyherbalism provides some advantages that single herbal formulations cannot match due to their synergistic

Received 7 October 2025; revised 14 February 2026; accepted 20 February 2026.
Available online 12 March 2026

* Corresponding author.
E-mail address: rifa123@ub.ac.id (M. Rifa'i).

https://doi.org/10.33640/2405-609X.3454

effects. This method can lower the possibility of unfavourable side effects by giving greater therapeutic efficacy at lower dosages. The formulation also showed fewer side effects and was environmentally friendly. Bioactive compounds derived from the individual plants are not enough to provide the pharmacological action [6].

Curcuma longa contains Curcumin, which has antioxidant activity with apoptotic and antiproliferative properties. Curcumin can alter the expression and functions of some proteins, including transcription factors, inflammatory cytokines, and enzymes, and gene products associated with cell survival and proliferation [7]. Furthermore, *Phyllanthus niruri* can inhibit breast cancer metastasis and proliferation by inhibiting matrix metalloproteinases 2 and 9 expression through the ERK pathway. Inhibiting hypoxia-inducible factor 1-α lowered the expression of vascular endothelial growth factor and inducible nitric oxide synthase, leading to anti-angiogenic effects and anti-metastasis [8]. Another herbal plant that has anticancer potential is *Ziziphus mauritiana,* or Indian jujube. This plant has anticancer agent activity, where the extracts from its fruits, leaves, and seeds show antioxidant activity, while its bark and pulp exhibit cytotoxic effects against various cancer cell lines [9]. Additionally, *Nigella sativa* also shows powerful anticancer ability and inhibits breast cancer cell migration, and promotes apoptosis [10]. In addition, *Annona muricata* Linn, or soursop, is a tropical plant with anticancer effects and is traditionally used worldwide to treat cancer. Studies show that its leaf and fruit extracts exert cytotoxic, chemoprotective, and anti-metastatic effects through mechanisms, such as cell cycle arrest, apoptosis, EGFR downregulation, and MAPK pathway modulation, primarily attributed to its rich acetogenin and alkaloid content [11].

EGFR plays a central role in cell physiology and oncogenesis, and extensive research has led to the development of effective targeted therapies. Additionally, EGFR is also known for driving proliferation and inhibiting apoptosis as a key proto-oncogene with complex signaling networks [12]. Furthermore, EGFR activation also begins with ligand-induced dimerization and cross-phosphorylation, creating docking sites for effector proteins that trigger primary signaling cascades, such as KRAS-MAPK, PI3K-AKT, and STAT, then driving proliferation, survival, angiogenesis, and migration, which are deregulated in cancer due to genetic mutations [13]. Another crucial pathway, such as mTOR, a kinase downstream of PIK3K/AKT, regulates cell growth through TORC1 and TORC2, and is frequently dysregulated in cancer. Hyperactivation of the PI3K/AKT/MTOR pathway can be driven by PIK3CA, AKT mutations, PTEN loss, or AKT2 amplification, which promote proliferation, survival, metastasis, and resistance to therapy [14]. This study aims to analyze the potential of polyherbal medicine in inhibiting the breast cancer proto-oncogene pathway.

2. Materials and methods

2.1. Sample preparation and liquid chromatography high-resolution mass spectrophotometry (LC-HRMS) analysis

The formulation of *C. longa, P. niruri, Z. mauritiana, N. sativa,* and *A. muricata* was obtained from Ismut Fitomedika Indonesia (IFI). The sample was prepared by weighing 5 mg in 1 mL of methanol, then filtered using a Nylon membrane with a pore size of 0.2 μm. LC-HRMS analysis was performed using UHPLC Vanquish™ Tandem Q Exactive Plus Orbitrap HRMS ThermoScientific™. ThermoScientific Accucore C18, 100 × 2.1 mm, 1.5 μm, was used for liquid chromatography. The mobile phase was analyzed using MS-grade water containing 0.1% formic acid (A) and acetonitrile + 0.1% formic acid (B) using a gradient method with a 0.2 mL/min flow rate. The mobile phase B was set at 5% and rose to 95% steadily in 28 min until returning to the previous state (5% B) for 28–33 min. The column temperature was 30 °C, and the injection volume was 2 μL. The untargeted screening was utilized with positive and negative ionization modes. The data was analyzed using the online database ChemSpider and mzCloud. Furthermore, the mass error of each compound was identified using Warwick Mass Error (https://warwick.ac.uk/fac/sci/chemistry/research/barrow/barrowgroup/calculators/mass_errors/), with a mass error score of up to ±10 ppm of the candidate structures, to ensure more accurate identification of bioactive compounds [15]. The fragment ions from compounds were determined using the database CFM-ID (Competitive Fragment Modeling Identification) (https://cfmid.wishartlab.com/) and FooDB (https://foodb.ca/) to predict, annotate, and understand the tandem mass spectra of small compounds [16]. The matched fragment ion from the database indicates similar bioactive compounds.

2.2. Drug-likeness, membrane permeability, bioactivity, and toxicity analysis

The bioactive compounds were screened using SwissADME (http://www.swissadme.ch/) with parameters Lipinski's rule of five, Veber, and Egan. Drug-likeness was determined through structural or physicochemical examinations of compounds that were progressed enough to be regarded as oral medication candidates. This concept is used to filter chemical libraries to exclude compounds having features that are most likely incompatible with an appropriate pharmacokinetic profile [17]. The compounds that passed drug-likeness screening were analyzed for toxicity screening using the ProTox web server (https://tox.charite.de/protox3/) to evaluate chemical safety and have the potential to manage risks associated with chemical exposure [18]. Membrane permeability screening was analyzed using the PerMM web server (https://permm.phar.umich.edu/) to determine compounds that are capable of diffusion through lipid bilayers [19]. The PerMM web server is utilized to calculate membrane binding energies, energy barriers, and permeability coefficients for various membrane systems [20]. Compounds that passed the screening were used for bioactivity analysis using the PASS Prediction of Activity Spectra for Substances web server (http://way2drug.com/passonline/). The biological activity was performed to determine Pa (to be active) and Pi (to be inactive) values using a cut-off value of Pa > 0.7 [21].

2.3. Target protein determination

Protein targets were determined using Swiss Target analysis (https://www.swisstargetprediction.ch/), Disgenet, and KEGG from DAVID (https://davidbioinformatics.nih.gov/tools.jsp). The protein was then analyzed for mutation using cBioportal (https://www.cbioportal.org/). The protein that showed more than 1% of mutation was used for further molecular docking analysis.

2.4. Functional annotation analysis

Functional annotation was performed to categorize target proteins according to their role in the cell. Functional annotation analysis was carried out using the DAVID web server (Database for Annotation, Visualization, and Integrated Discovery) (https://david.ncifcrf.gov/) [22]. The databases were created using the Gene Ontology (GO) and the Kyoto Encyclopedia of Genes and Genomes (KEGG pathway). GO groups proteins into three domains: Biological Process, Cellular Component, and Molecular Function. The KEGG pathway classifies target proteins based on their role in human cellular pathways [23].

2.5. Protein and ligand preparation

PubChem was utilized to obtain the 2D structure of the compounds (https://pubchem.ncbi.nlm.nih.gov/). The 3D structure of compounds was used for molecular docking analysis. The inhibitors for the proteins were obtained from PubChem or extracted from the protein PDB using Discovery Studio 2019. The ligands are then minimized using the Open Babel plugin built into the PyRx 0.9.5 program. Furthermore, the RCSB PDB database was utilized to retrieve the 3D structure of the protein target (https://www.rcsb.org/) (Table 1). The protein was prepared using Discovery Studio 2019 Client ver 19.1.0 software (Dassault Systèmes Biovia, San Diego, California, USA) by removing water molecules and native protein ligands. The results obtained were saved in PDB format.

2.6. Molecular docking and visualization

Specific docking to the active areas of the protein target was performed using AutoDock Vina tools and PyRx 0.9.5 (Table 1). The complex with the lowest binding affinity compared to the inhibitor was chosen for the molecular dynamics simulation.

2.7. Molecular dynamics and binding energy simulation

Molecular dynamics analysis was carried out using Yet Another Scientific Artificial Reality Application (YASARA) 19.12.14 version. The AMBER14 force field was used on YASARA Dynamics for the simulation. Furthermore, water molecules were added, and then the system was neutralized with 0.9% NaCl salt at 310 K and pH 7.4. The simulation was carried out under a periodic boundary condition. The temperature of the simulation was regulated by the Berendsen thermostat (310 K) and barostat (1 pressure bar) for 20 ns with automated storage every 25 ps. The simulation was performed with the macro program md_runfast. Additionally, the analytical program md_analyze was utilized to compute root-mean-square deviation (RMSD), spin radius, and hydrogen bonds. The root mean square fluctuation (RMSF) was analyzed using md_analyzeres, and the molecular dynamic binding energy was analyzed using md_bindingenergy [24].

Table 1. Polyherbal medicine bioactive compounds and the matched fragment ions.

No	Compound	Formula	RT (min)	Theoretical *m/z*	Observed *m/z*	Mass error (ppm)	CID	Fragment ion *m/z*	Bioavailability
1	Curcumin	$C_{21}H_{20}O_6$	16.758	368.12477	369.13117	−4.346352	969516	368.1240; 369.13171	0.55
2	Curcumin II	$C_{20}H_{18}O_5$	16.45	338.11443	339.12122	−3.57867	5469424	91.05421; 121.06499; 117.0322; 119.048; 145.02808; 147.04370; 339.12155	0.55
3	Hexyl cinnamaldehyde	$C_{15}H_{20}O$	20.786	216.15079	217.15807	−3.3331008	1550884	83.04924; 91.05438; 103.05437; 117.06985; 119.08537; 217.15834	0.55
4	DL-malic acid	$C_4H_6O_5$	1.117	134.02049	133.01321	5.72313	525	59.013; 71.01279; 72.99207; 87.00768; 89.02341; 115.00268; 133.01332	0.56
5	Choline	$C_5H_{13}NO$	1.049	103.09983	104.10711	−6.983523	305	58.06557; 60.08119; 86.09664; 104.10690; 105.11031	0.55
6	(+)-Nootkatone	$C_{15}H_{22}O$	22.38	218.16635	219.17369	−3.025214	1268142	53.03899; 79.05452; 93.07001; 91.05426; 105.06985; 177.12672; 201.16341; 219.17371	0.55
7	L-(+)-Valine	$C_5H_{11}NO_2$	1.052	117.07894	118.08621	−6.25109	6971018	54.50256; 56.04974; 58.06556; 59.07337; 70.06546; 116.07059; 118.08608	0.55
8	4-Aminobenzoic acid	$C_7H_7NO_2$	1.079	137.04744	138.05472	−5.253655	978	67.05454; 78.03426; 93.05777; 93.05267; 92.04962; 94.06527; 111.06344; 138.05460	0.55
9	1,3,4,5-Tetrahydroxycyclohexanecarboxylic acid	$C_7H_{12}O_6$	1.075	192.06256	191.05528	3.748779	1064	57.03351; 59.01273; 71.01273; 85.02848; 87.00786; 127.03931; 171.02898; 173.04494; 191.05542; 192.05869	0.56
10	Valerenic acid	$C_{15}H_{22}O_2$	16.311	234.16113	235.16841	−3.074806	6440940	67.0546; 81.07013; 107.08566; 109.10123; 217.15805; 235.16861	0.85
11	Pulcherriminic acid	$C_{12}H_{20}N_2O_4$	16.31	256.14305	257.15033	−2.810929	3083664	57.07036; 71.08572; 171.04346; 257.15045	0.55
12	Moracin C	$C_{19}H_{18}O_4$	15.925	310.11992	309.11292	3.224559	155248	203.07089; 309.11322	0.55
13	Phytosphingosine	$C_{18}H_{39}NO_3$	15.386	317.29192	318.29919	−2.30072	122121	71.08589; 300.28900; 318.29950	0.55
14	13S-hydroxyoctadecadienoic acid	$C_{18}H_{32}O_3$	19.936	296.23469	295.22742	2.464262	6443013	59.01278; 113.09597; 195.13841; 277.21713; 296.23090; 295.22757	0.85
15	Pheophorbide A	$C_{35}H_{36}N_4O_5$	26.631	592.26561	593.27289	−1.215671	253193	533.25458; 593.27399	0.56
16	(+)-Alantolactone	$C_{15}H_{20}O_2$	16.91	232.14557	233.15285	−3.101502	72724	79.05446; 91.05434; 107.08559; 177.09061; 233.15334	0.55
17	Sphinganine	$C_{18}H_{39}NO_2$	17.62	301.29689	302.3041	−2.621999	91486	57.0703; 71.08588; 102.09145; 284.29376; 303.30789; 302.30444	0.55
18	Cinnamyl alcohol	$C_9H_{10}O$	17.732	134.07288	135.08015	−5.4448	5315892	65.03346; 65.03877; 91.05444; 117.06985; 135.08023	0.55
19	Linolenelaidic acid	$C_{18}H_{30}O_2$	19.96	278.22353	279.23074	−2.839444	5282822	55.05460; 67.05458; 69.07025; 79.05442; 81.07012; 83.08594; 131.08531 93.07005; 95.08564; 107.08572; 109.10115; 131.08531; 149.13223;	0.85
20	Reticuline	$C_{19}H_{23}NO_4$	7.715	329.16146	330.1687	−2.308897	439653	137.05945; 151.07527; 192.10152; 299.12653; 330.16925	0.55
21	5,7,4′-Trihydroxy-6-prenylflavanone	$C_{20}H_{20}O_5$	16.192	340.1302	339.12314	2.76648	3519901	120.05250; 119.04922; 134.0632; 149.05991; 191.07008; 219.06673; 233.08058	0.55
22	Azelaic acid	$C_9H_{16}O_4$	9.725	188.10408	187.0968	3.827668	2266	57.03357; 97.06486; 125.09618; 143.10680; 187.09683; 188.10062	0.85

(*continued on next page*)

Table 1. (continued)

No	Compound	Formula	RT (min)	Theoretical *m/z*	Observed *m/z*	Mass error (ppm)	CID	Fragment ion *m/z*	Bioavailability
23	2-Butylfuran	$C_8H_{12}O$	23.37	124.08859	125.09587	−5.802306	20534	55.05468; 59.04943; 67.05453; 69.03385; 79.05450; 83.04935; 97.06499; 107.08559; 109.06494; 125.09594	0.55
24	L-(+)-Leucine	$C_6H_{13}NO_2$	1.584	131.09447	132.10168	−6.026189	6106	69.07024; 86.09664; 132.10164	0.55
25	Benzoic acid	$C_7H_6O_2$	6.992	122.03573	121.02846	5.981855	243	121.0285; 122.03168	0.85
26	Curcumene	$C_{15}H_{22}$	20.481	202.17148	203.17876	−3.561333	92139	55.05465; 67.05455; 79.05447; 69.07014; 81.07010; 93.06999; 91.05440; 95.08562; 107.08557; 105.06990; 119.08540; 147.11646; 161.13206;	0.55
27	Annonacin	$C_{35}H_{64}O_7$	24.647	596.46373	597.47101	−1.207114	354398	67.05457; 95.08566	0.55
28	D-Glucopyranuronic acid	$C_6H_{10}O_7$	1.062	194.04187	193.03459	3.710539	94715	59.01273; 87.00786; 103.00272	0.56

3. Results

3.1. Identification of bioactive compounds in polyherbal formulation

LC-HRMS analysis was performed to identify bioactive compounds in the polyherbal medicine. The mass error and fragmentation ion of each compound were analyzed using Warwick mass error calculation (https://warwick.ac.uk/fac/sci/chemistry/research/barrow/barrowgroup/calculators/mass_errors/). The study showed that there were 28 compounds identified according to the CFM-ID Database (https://cfmid.wishartlab.com/) and met the criteria between −10 and 10 ppm of mass error (Table 1).

The compounds' fragment ions were compared with the database, revealing several matched fragment ions. CFM-ID is a machine learning tool to predict *in silico* tandem mass spectra (MS/MS) for suspected metabolites, for which the chemical standards are not available [25]. The database accurately predicts electrospray ionization mass spectra (ESI-MS/MS) from chemical structure, then identifies compounds according to MS/MS spectral matches [26].

A previous study showed the LC-HRMS fractionation result of *Curcuma longa* contained curcumin, dimethoxycurcumin, and curcumene, which were also included in our present study [27]. In addition, *P. niruri* in previous literature also demonstrated several compounds similar to those in our previous study, such as azelaic acid [28]. *A. muricata* also displayed annonacin, which is consistent with the LC-HRMS profiles of *A. muricata* [29]. Furthermore, a previous study also explained about *Z. mauritiana* compounds such as D-Glucopyranuronic acid, which were included in the present study. The compound is well known for liver detoxification and excreting glucuronidation as an exogenous chemical [30].

3.2. Drug-likeness screening, membrane permeability, bioactivity, and toxicity analysis

Drug-likeness screening was conducted to analyze which compounds have a role as medicine. In addition, drug-likeness, introduced to guide advanced drug discovery, refers to the molecular physicochemical properties typical of drugs and often linked to PK and safety, also identifies compounds with desirable ADMET properties using Lipinski's Rule of Five, Veber, and Egan analysis that define compounds within specific property ranges as drug-like [31]. According to the study of

drug-likeness screening, 21 bioactive compounds pass the Lipinski, Veber, and Egan properties (Fig. 1A). The drug-likeness screening also showed that all phytochemicals showed more than 0.55 in bioavailability scores. Phytochemicals with a bioavailability score≥ 0.55 are considered easy and are well absorbed by the body [32]. Drug-likeness requires assessing a compound's absorption, distribution, metabolism, and excretion (ADME). In addition, this analysis plays a crucial role in maintaining the balance of molecular characteristics and structural traits. The Lipinski rule of five was used to assess drug-likeness according to five physicochemical properties, and evaluates the bioavailability of bulk materials to determine their drug-like qualities [33].

The membrane permeability analysis indicates that every 21 compounds can penetrate the plasma membrane (Fig. 1B). PerMM analysis was performed to calculate membrane binding energies, energy barriers, and permeability coefficients for various membrane systems [20]. This will identify the passive permeability of molecules across membranes with diverse structures. Passive diffusion requires the movement of molecules in response to the concentration gradient between the two water media on the two sides of the membrane sides [34].

Bioactivity analysis was conducted to determine compounds with potential anticancer activity. In addition, the screening identified five compounds with the highest potential, such as curcumin, curcumin II, moracin C, 5,7,4′-Trihydroxy-6-prenylflavanone, and D-Glucopyranuronic acid (Fig. 2A). The compounds curcumin, curcumin II, moracin C, and 5,7,4′-Trihydroxy-6-prenylflavanone possess apoptotic agonist properties. In addition, an important property demonstrated is the free radical scavenger activity possessed by all five compounds. Furthermore, the compound 5,7,4′-Trihydroxy-6-prenylflavanone showed optimal activity in MMP9 and TP53 expression, antineoplastic, and antimutagenic activities. Polyherbal bioactive compounds undergo enzymatic digestion, metabolic modification, and selective absorption before exerting biological effects. The analysis in this study was intended to illustrate the analytical and experimental screening strategy.

Additionally, the toxicity prediction of bioactive compounds showed that the five compounds are unlikely to cause liver and nervous system damage. According to the carcinogenicity property, they were also predicted as inactive with a probability of 0.95, so they are unlikely to be carcinogens. The mutagenicity aspect showed that they did not cause genetic mutations. In addition, the cytotoxicity property was predicted as inactive, and the compounds are not toxic to the cells (Fig. 2B). Furthermore, the LD50 analysis showed that the bioactive compounds exhibit low acute toxicity. Curcumin, Curcumin II, and 5,7,4′-Trihydroxy-6-prenylflavanone can be harmful in high quantities. Additionally, moracin C is safer and may be harmful at extremely large doses. In addition, D-Glucopyranuronic acid is nontoxic to humans (Fig. 2C).

3.3. Target protein compounds of polyherbal formulations

The protein target analysis was conducted to determine the appropriate target protein for each compound. The study was performed to identify the protein targets of each compound. Swiss Target is a database used to identify potential protein targets by inputting SMILES structures. In addition, Disgenet and KEGG were used to screen target proteins from the Swiss Target to make them more specific. Furthermore, cBioportal was used to identify mutations in the target proteins, where if mutations of more than 1% were found, they would be used as target proteins for molecular docking.

The study showed that curcumin has several target proteins, such as EGFR and AKT1, while the curcumin II compound also has the MTOR protein. Additionally, the bioactive compound moracin C can target several compounds, such as AKT1 and ESR1. In addition, 5,7,4′-Trihydroxy-6-prenylflavanone also targets the ESR1 protein and other proteins such as PIK3CA, ERBB2, and KIT. Furthermore, the last compound, D-Glucopyranuronic acid, shows the protein AKT1 and ESR1 as the target (Fig. 3).

Swiss Target Prediction is a vital database to predict compound targets according to the similarities of compounds' structures. The database assigns a score to each target to indicate the likelihood of a target protein prediction [35]. CBioPortal was utilized as a comprehensive resource for patients and sample-level clinic genomic data in cancer, enabling detailed studies and comparisons of different subtypes. Furthermore, this database offers efficient analysis, making it ideal for researchers without prior knowledge of massive datasets [36]. The cBioPortal database can assess the genetic alterations in such proteins, specifically in cancer disease. Genetic mutations are crucial to predict and understand disease, especially in breast cancer [37]. Furthermore, the protein–protein interaction (PPI) network was analyzed using the six molecular targets of the polyherbal medicine

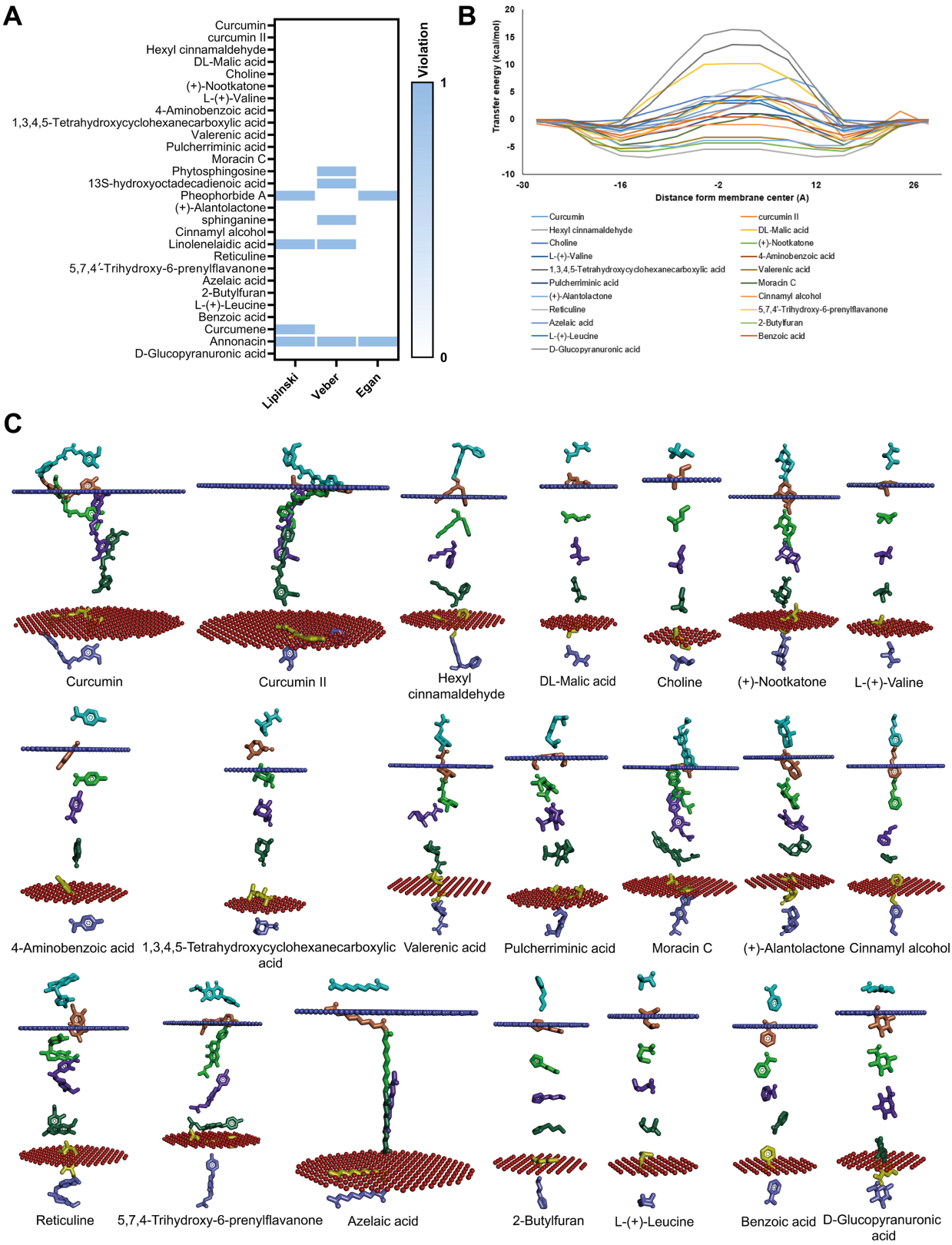

Fig. 1. Polyherbal bioactive compound screening as a conceptual schematic of the screening workflow. A. Drug-likeness analysis, B. Transfer energy in membrane permeability, C. Visualization of membrane permeability analysis.

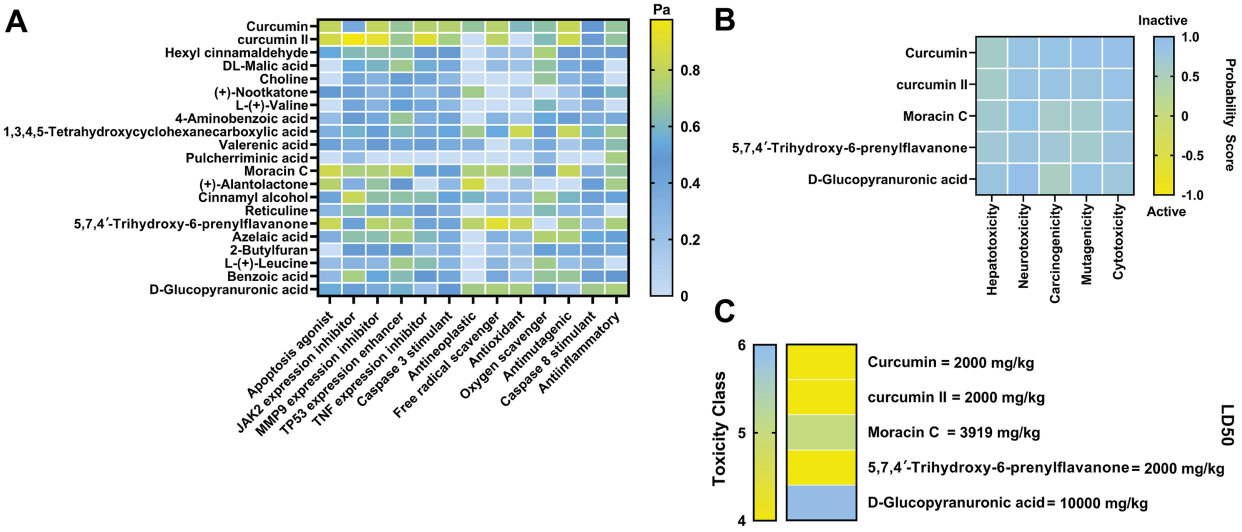

Fig. 2. Polyherbal bioactive compound screening. A. Bioactivity analysis, B. Toxicity probability score, C. Toxicity class prediction.

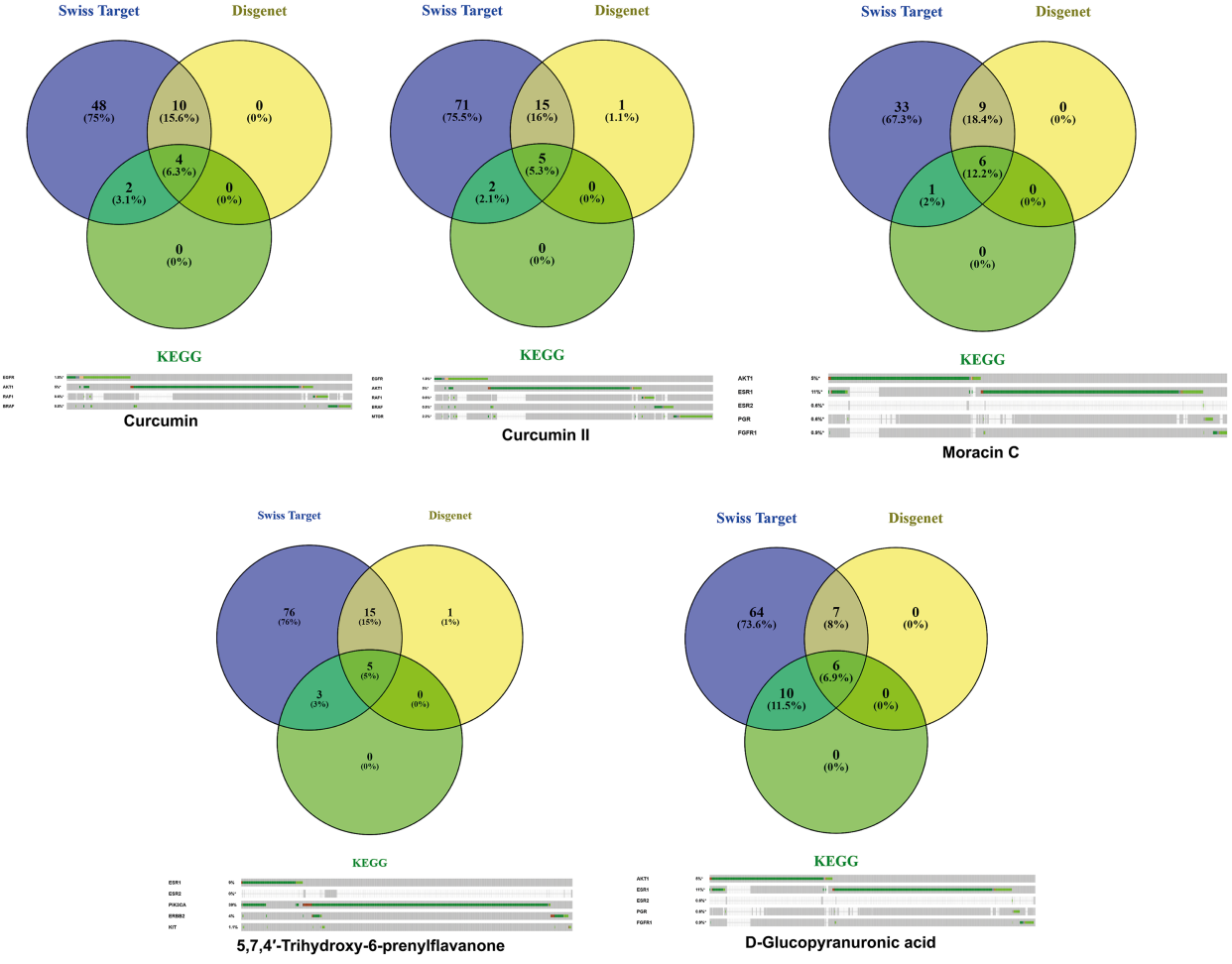

Fig. 3. Protein target prediction of each selected compound.

(Fig. 4A). Signalling route cross-talk demonstrated the therapeutic effect. The highest connections were shown by highlighted yellow proteins, such as EGFR, PIK3CA, AKT1, ERBB2, MTOR, and ESR1. The result indicates their crucial regulatory roles in the network.

Proteins associated with the upstream signaling, such as IGF1R and the ERBB family [38,39]. In addition, intracellular kinases demonstrate several proteins, such as PI3K isoforms, SRC, JAK3, and PTK6 [40–42]. Additionally, downstream effectors contribute with STAT1/3 and CCND1, then form interconnected modules converging primarily on the PI3K/AKT/mTOR pathway [43]. The PPI network displayed that the bioactive compounds targeted a multi-node, multi-pathway regulatory system rather than a single pathway.

Gene ontology analysis was performed for biological process, cellular component, and molecular function roles (Fig. 4B). The protein network showed several proteins associated with signal transduction, including 37 proteins, the EGFR signaling pathway, and intracellular signal transduction for 21 proteins, indicating central regulators of upstream and downstream signaling cascades. In addition, cell proliferation, positive regulation of apoptotic signaling, MAPK cascade, and T-cell receptor signaling are also represented, suggesting that this network modulates key pathways in cell growth and immune regulation.

The proteins are also localized in the cytosol, plasma membrane, and cytoplasm, which indicates the dominance of kinase adaptors and receptors. Furthermore, molecular function analysis demonstrates protein binding, ATP binding, protein kinase activity, and receptor-tyrosine kinase binding. High representation of protein serine/threonine kinase activity and enzyme binding indicates the key regulators of PI3K/AKT, MAPK, and JAK/STAT pathways.

3.4. Molecular docking between compounds from polyherbal formulations and their target proteins

Molecular docking analysis was performed and showed various binding affinities and a similar position of chemical interaction compared to the inhibitor (Table 2, Fig. 5). EGFR interacting with curcumin showed similarity in hydrophobic interaction, such as ALA743 and LEU844, compared to the inhibitor. In addition, curcumin II interacts with EGFR and indicates two similar hydrophobic interactions with the inhibitor, such as VAL726 and LYS745. Additionally, curcumin II exhibited lower binding affinity after interacting with MTOR compared to the inhibitor, which is −8.5 kcal/mol. The amino acid residue also showed a similar position compared to the inhibitor, which are TYR1583 and LYS1452.

Furthermore, moracin C interacts with protein ESR1 and displays similar amino acid residues for hydrophobic interaction, such as ALA350, LEU525, and LEU387. Moreover, 5,7,4′-Trihydroxy-6-prenylflavanone with PIK3CA exhibited low binding affinity, which is −9.2 kcal/mol, and there is one hydrogen interaction and three hydrophobic interactions compared to the inhibitor. Protein ESR1 interacts with compound D-Glucopyranuronic acid and indicates two similar hydrogen interactions compared to the inhibitor, such as ARG394 and GLU353.

3.5. Interaction between compounds in polyherbal medicine and their target proteins

A molecular dynamics simulation was performed to demonstrate the interaction stability between the ligand and protein. The simulation was determined using RMSD backbone, number of hydrogen bonds, and binding energy analysis (Fig. 6). RMSD backbone analysis showed a stable simulation in curcumin with EGFR, since the RMSD value is less than 3 Å, whereas curcumin II is less stable because the RMSD value is mostly more than 3 Å. In addition, curcumin II also interacts with MTOR and is more stable compared to the EGFR interaction. Furthermore, the interaction exhibited instability in the middle and at the end of the simulation. Moracin C, D-Glucopyranuronic acid, and 5,7,4′-Trihydroxy-6-prenylflavanone showed more stability in the simulation from the start to the end of the simulations since the RMSD values are less than 3 Å. Ligands with lower RMSD values (<3 Å) remained more stable in the initial pose, while an average RMSD of 3–8 Å indicated that the ligand underwent conformational changes while binding and was stable in the catalytic site [44] (Fig. 6A).

Moreover, the number of hydrogen bonds was also analyzed, and it was shown that curcumin and curcumin II have more hydrogen bonds compared to their inhibitor in EGFR and MTOR interaction. Furthermore, moracin C and 5,7,4′-Trihydroxy-6-prenylflavanone have fewer hydrogen bonds compared to their inhibitors. In contrast, D-Glucopyranuronic acid has a greater number of hydrogen bonds compared to the inhibitor in the simulation (Fig. 6B).

The binding energy simulation also determines the stability of ligand and macromolecule interaction. The simulation demonstrated that curcumin, curcumin II, moracin C, D-Glucopyranuronic acid,

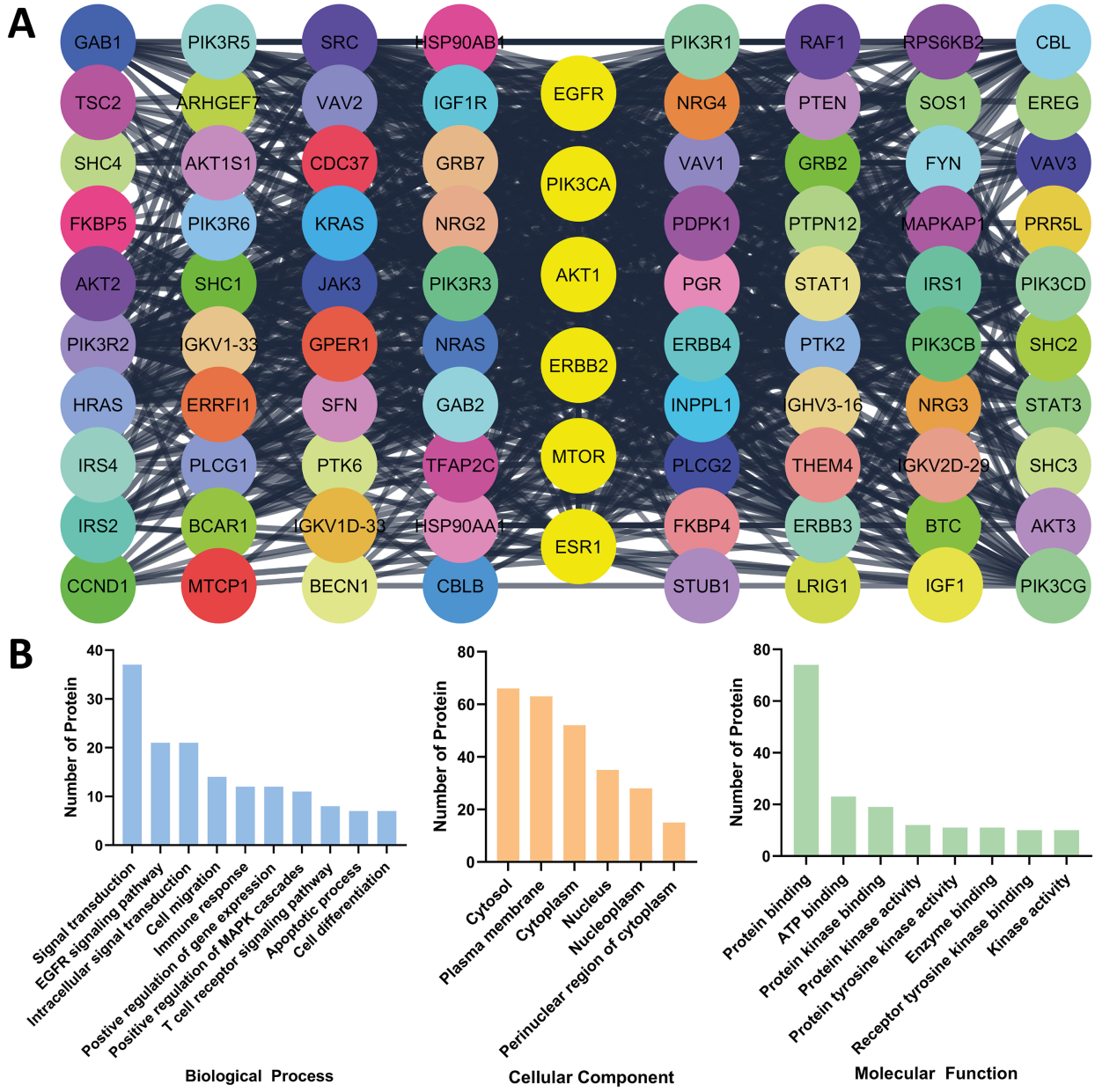

Fig. 4. Functional annotation analysis of the protein targets. A. Protein–protein network examination and B. Gene ontology determination of biological process, cellular component, and molecular function.

and 5,7,4′-Trihydroxy-6-prenylflavanone showed more negative binding energy compared to their inhibitor. On the other hand, curcumin II showed higher binding energy compared to the inhibitor when it interacts with MTOR (Fig. 6C).

4. Discussion

4.1. Polyherbal medicine bioactive compounds

Polyherbal medicine showed potential bioactive compounds such as curcumin, curcumin II, moracin C, 5,7,4′-Trihydroxy-6-prenylflavanone, and D-Glucopyranuronic acid. Curcumin is a hydrophobic polyphenol from *Curcuma longa.* It has long been used in traditional medicine and is highly recognized for its anticancer role by regulating multiple signaling pathways, including transcription factors, receptors, kinases, cytokines, enzymes, and growth factors. Moreover, clinical and experimental studies have demonstrated its efficacy, such as in mammary cancer, highlighting curcumin as a promising agent for cancer prevention and therapy in combination or alone [45]. Curcumin II or

Table 2. Molecular docking analysis of bioactive compounds with the targeted protein and inhibitor.

Compound	Protein Target	PDB ID	Inhibitor	Binding affinity (kcal/mol)	
				Protein-compound	Protein-inhibitor
Curcumin	EGFR	4I23	Dacomitinib	−7.4	−8.1
	AKT1	6HHF	Borussertib	−9.1	−15.2
Curcumin II	EGFR	4I23	Dacomitinib	−7.6	−8.1
	AKT1	6HHF	Borussertib	−9.1	−15.2
	MTOR	4JSV	Inhibitor	−8.5	−7.8
Moracin C	AKT1	6HHF	Borussertib	−9.5	−15.2
	ESR1	3ERT	Tamoxifen	−7.8	−9.8
5,7,4′-Trihydroxy-6-prenylflavanone	ESR1	3ERT	Tamoxifen	−7.2	−9.8
	PIK3CA	5DXT	Alpelisib	−9.2	−9.7
	ERBB2	3PP0	Inhibitor	−10.4	−11.1
	KIT	7KHG	Pexidartinib	−9.6	−11.9
D-Glucopyranuronic acid	AKT1	6HHF	Borussertib	−5.7	−15.2
	ESR1	3ERT	Tamoxifen	−6.1	−9.8

desmethoxycurcumin is contained in *Curcuma longa* and showed anticancer activity (anticarcinogenic) in moderate criteria (0.5 < Pa < 0.7) [46].

Moracin C is a phenolic compound that shows anti-inflammatory activity and potentially inhibits the proliferation of the A549 cell line and the human breast cancer cell line MCF-7 [47]. Additionally, moracin C also exhibited the most potent cytotoxicity against the HL-60 cell line or human leukemia cells with an IC50 value of 6.7 ± 0.8 μM [48]. In addition, 5,7,4′-Trihydroxy-6-prenylflavanone is a flavonoid derivative that has a prenyl side chain, which increases the structural diversity of flavonoids and enhances their bioactivity and bioavailability. This compound exhibits anticancer, anti-inflammatory, neuroprotective, anti-obesity, anti-diabetic, and cardioprotective properties [49]. This study, as a preliminary screening to

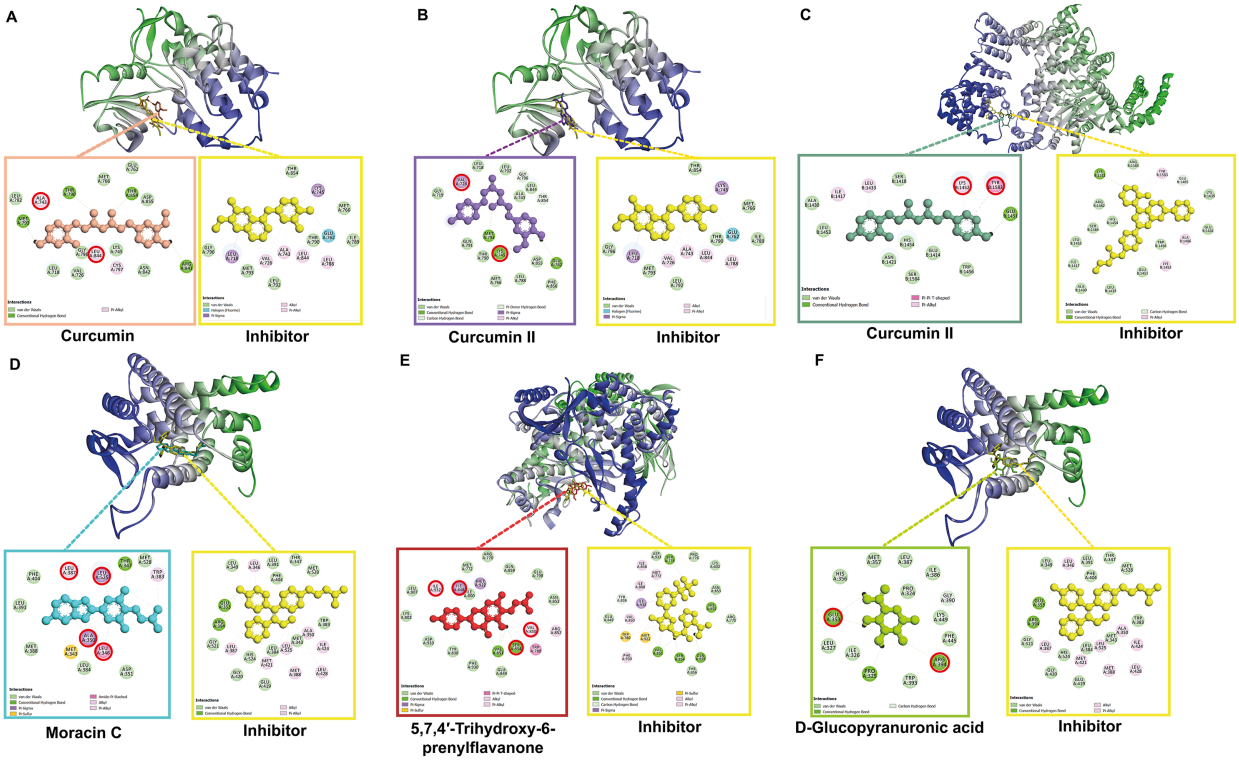

Fig. 5. Molecular docking visualization and position of chemical interaction. A. EGFR-Curcumin and EGFR-Inhibitor, B. EGFR-Curcumin II and EGFR-Inhibitor, C. MTOR-Curcumin II and MTOR-Inhibitor, D. ESR1-Moracin C and ESR1-Inhibitor, E. PIK3CA-5,7,4′-Trihydroxy-6-prenylflavanone and PIK3CA-Inhibitor, F. ESR1-D-Glucopyranuronic acid and ESR1-Inhibitor. Note: A Red circle means the similarity of the compound's position in the chemical interaction with the inhibition.

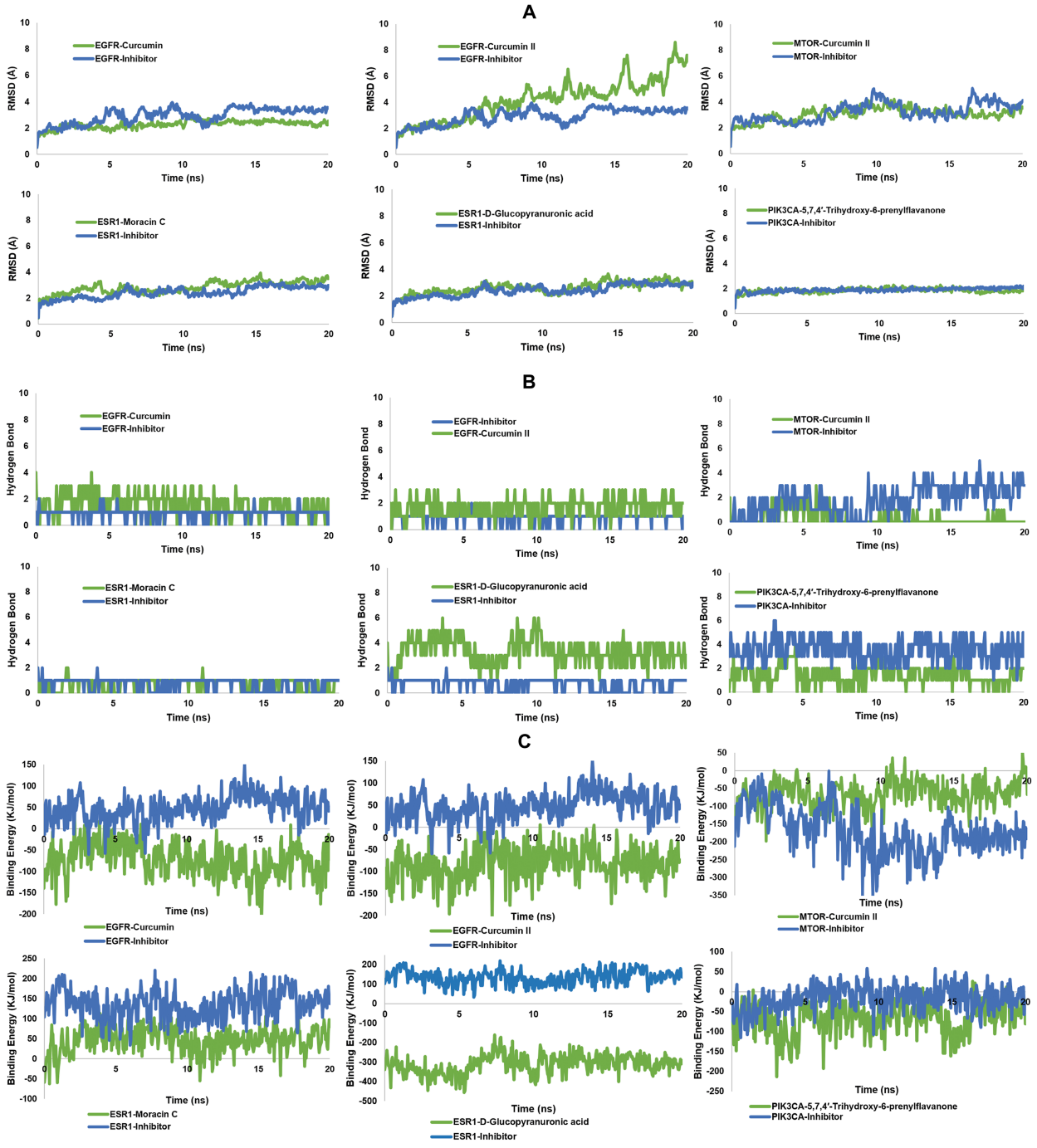

Fig. 6. Molecular dynamics simulation result of compounds with each target protein. A. Root-mean-square deviation (RMSD) backbone, B. The number of hydrogen bonds and the C. Binding energy simulation.

characterize the bioactive compounds, has a limitation of the absence of chromatographic fractionation to isolate individual compounds. Future studies will incorporate solvent extraction followed by fractionation-based isolation and subsequent LC-HRMS analysis of the fraction. This approach will enable more precise identification of active metabolites. Fractionation-based analysis would strengthen compound-specific validation in future research.

The molecular docking analysis displayed only single-compound interactions. It does not account for the synergistic, additive, or antagonistic effects that may occur when metabolites are combined within the polyherbal formulation. Further *in vitro* examination is required for the extract or fractions.

4.2. Drug-likeness potential, membrane permeability, bioactivity, and toxicity screening

The screening analyses indicated the identification of compounds with suitable ADME characteristics, membrane permeability, functional relevance, and acceptable toxicity profiles. Incorporating these steps improves the transparency and rationale of the molecular docking analysis. The drug-likeness analysis identifies that the five compounds had no violation in the Lipinski, Veber, and Egan parameters. Understanding and predicting oral bioavailability for an orally administered drug is essential. The absorption and distribution of drugs in the body significantly impact their therapeutic efficacy [50]. Additionally, membrane permeability analysis also indicates that the potential compound exhibited low transfer energy and can penetrate the membrane lipid bilayer. Membrane permeability is an essential parameter in drug development. A drug must have sufficient permeability with high efficacy for the intracellular target [51].

Curcumin and curcumin II have several significant bioactivities that play a crucial role in breast cancer, such as apoptosis agonist, MMP9 and TNF expression inhibitor, free radical scavenger, antimutagenic, and caspase 3 stimulant. In addition, moracin C and 5,7,4′-Trihydroxy-6-prenylflavanone also showed apoptosis agonist, MMP9 and TNF expression inhibitor, antineoplastic, and free radical scavenger. Moreover, 5,7,4′-Trihydroxy-6-prenylflavanone simulates antioxidant, antimutagenic, and anti-inflammatory activities. Furthermore, D-Glucopyranuronic acid displays other potentials, such as a caspase 8 stimulant. These bioactivities have a Pa value > 0.7 as the cut-off. Pa value denotes the compound's active nature, while Pi symbolizes its passive nature. Pa value with more than 0.7 means that the bioactive compounds are likely to have considerable experimental, biological, and pharmacological activity [52].

The five compounds also showed non-toxic and safe results for humans according to parameters of hepatotoxicity, neurotoxicity, carcinogenicity, mutagenicity, and cytotoxicity. This result indicates that the bioactive compounds are safe for the liver and neurons, non-carcinogenic, non-mutagenic, and non-toxic. Drug-induced neurotoxicity can potentially cause severe difficulties in the regular functioning of the brain, resulting in a variety of neurological symptoms or diseases [53]. These screens have limitations and can be used to analyze compound prioritization.

4.3. Determining the protein target in breast cancer

Protein targets were determined explicitly according to each compound. EGFR was targeted, and the protein interacts with curcumin and curcumin II. Additionally, AKT1 interacts with curcumin, curcumin II, moracin C, and D-Glucopyranuronic acid. MTOR also interacts with curcumin II; meanwhile, moracin C and D-Glucopyranuronic acid interact with ESR1. In addition, PIK3CA, ERBB2, and KIT interact with 5,7,4′-Trihydroxy-6-prenylflavanone. Those proteins play an essential role in breast cancer. The epidermal growth factor receptor (EGFR) is widely regarded as the prototype for all receptor tyrosine kinases. In addition, this protein is one of the ERBB family receptor tyrosine kinases that play a crucial role in epithelial cell physiology. EGFR is frequently mutated or overexpressed in various cancers, including breast cancer [54,55].

Protein kinase inhibitors (PKIs) are therapeutic agents designed to block the activity of protein kinases. PKIs work by competing with ATP at the catalytic site, while others bind in a form that forms covalent bonds to enhance selectivity and durability of inhibition. In addition, EGFR and PI3K/Akt/mTOR pathway illustrate how kinase dysregulation drives cancer. EGFR inhibitors suppress downstream RAS-RAF-MEK-ERK signaling to reduce proliferation, but resistance can arise through secondary mutation or activation of bypass routes, such as PI3K/Akt. Furthermore, hyperactivation of AKT and mTOR promotes survival and growth, often through mutations in regulators, such as PIK3CA or TSC1/2 [56,57]. ERBB2 promotes tumor progression and chemoresistance; therefore, this protein is essential to suppress in breast cancer therapy. In addition, ERBB2 is overexpressed in about 30% of breast cancer cases and is strongly associated with aggressive behavior, metastasis, and poor clinical outcomes [58].

The present study contributes to supporting the therapeutic potential of natural bioactive compounds as kinase-targeting agents in breast cancer. Bioactive compounds from herbal medicine modulate critical oncogenic pathways, including EGFR, PI3K/Akt/mTOR. Our study found that curcumin, curcumin II, moracin C, D-Glucopyranuronic acid, and 5,7,4′-Trihydroxy-6-prenylflavanone modulate key nodes within these pathways, suggesting they may function as a selective inhibitor and play an essential role in a broader multi-pathway suppression strategy.

The protein–protein network analysis showed that the bioactive compounds in the polyherbal

medicine act via multi-target modulation of interconnected pathways, dominating growth factor receptor signaling and PIK3/AKT/mTOR pathway. Gene ontology enrichment analysis indicates that bioactive components predominantly influence pathways in cell survival, proliferation, and inflammatory response. The cytosolic and membrane-localized proteins in the CC analysis align with receptor-mediated signaling, where ligand binding at the cell surface can trigger downstream phosphorylation activity in the cytosol [59]. Furthermore, MF enrichment in ATP binding, kinase activity, and receptor-kinase binding confirms that the network is driven by enzymes, scaffold proteins, and receptor complexes, which play a crucial role as checkpoints.

PI3Kinase (PI3K) activates AKT1 by phosphorylating phosphatidylinositol 4,5-biphosphate (PIP2), resulting in phosphatidylinositol 3,4,5-triphosphate (PIP3) [60]. Moreover, mTOR is a serine/threonine protein kinase that is located downstream of the PI3K and AKT pathway [61]. Most breast cancers (≥80%) are hormone-dependent, commonly expressing ER, especially ESR1, PR, and/or HER, which drive their growth. ESR1 is activated by estrogen and plays a role in tumor progression [62].

4.4. Molecular docking analysis exhibited low binding affinity and similar chemical interaction position

Molecular docking analysis showed that 5,7,4′-Trihydroxy-6-prenylflavanone exhibited a favorable binding affinity toward PIK3CA. Hydrogen bonds were established with VAL851 and SER854, then hydrophobic interactions with ILE838, ILE932, VAL850, ARG852, and TRP780, similar to alpelisib's active sites. The analysis is particularly significant since PIK3CA is one of the most frequently mutated oncogenes in breast cancer.

Similarly, curcumin II displayed low binding affinity toward MTOR. These results suggest that some bioactive compounds may achieve interaction energies comparable to clinically used inhibitors. In addition, the chemical interaction position also revealed that ligands established multiple hydrogen bonds and hydrophobic interactions with amino acid residues critical for the stability of each active site. Furthermore, similarity in binding residues between bioactive compounds and inhibitors indicates competitive binding potential. Although D-Glucopyranuronic acid exhibited moderate binding affinity (−5.7 kcal/mol) against AKT1, it still formed stable hydrogen bonds, such as ARG394 and GLU353, which are critical for maintaining the ESR1 structural conformation.

Moreover, structure similarity suggests that bioactive compounds have a similar pocket and potentially interfere with the same signaling cascade as the inhibitor. This study indicates that phytochemicals such as curcumin II, moracin C, and 5,7,4′-Trihydroxy-6-prenylflavanone demonstrate promising binding profiles against oncogenic target proteins. The molecular docking analysis also suggests that curcumin II shows slightly stronger affinity compared to curcumin itself.

Curcumin and curcumin II with EGFR showed interactions that align strongly with the residues. Hydrophobic pocket residues can enhance the ligand binding via van der Waals interactions, such as ALA743 and LEU844 for curcumin (Fig. 5A), then VAL 726 for curcumin II (Fig. 5B). In addition, LYS745 showed strong interaction in the hydrogen-bond network with the EGFR inhibitor. Curcumin forms a hydrogen-bond interaction with LYS745, suggesting a stabilizing anchoring in the catalytic site.

Curcumin II binds to MTOR and shows critical interacting residues, such as LYS1452 and TYR1583. These residues are located on the ligand surface and at the edge of the binding channel. Furthermore, they contribute to the secondary electrostatic stabilization and define the ligand entry or exit pathway (Fig. 5C). Moreover, moracin C and the inhibitor within ESR1 show that both ligands occupy the canonical ligand-binding pocket and interact with a largely overlapping set of key residues. Hydrophobic contacts with LEU387, LEU525, ALA350, and LEU346 stabilize Moracin C, forming a non-polar environment that anchors its aromatic rings. The presence of these shared interactions suggests that Moracin C occupies the same functional cavity as the established ESR inhibitor (Fig. 5D).

The binding profile of 5,7,4′-Trihydroxy-6-prenylflavanone within PIK3CA demonstrates that the ligand interacts with several residues that are likewise engaged by the reference inhibitor. Both ligands share hydrophobic amino acids with ILE932, ILE848, VAL850, and one hydrogen bond for SER854 (Fig. 5E). The π-alkyl interaction with ILE932 and VAL850 stabilizes the aromatic scaffold within the catalytic region. In addition, the non-polar pocket consists of ILE848, frequently utilized by ATP-competitive PI3K. Additionally, SER854, as a hydrogen bond amino acid, can stabilize the interaction and be involved in ligand orientation. The matched amino acid interactions indicate that the compound occupies the same functional binding pocket and may exhibit a similar ATP-competitive inhibitory mechanism against PIK3CA. In

addition, GLU353 and ARG394 are the residues that form strong hydrogen bond anchors in ESR1-D-glucopyranuronic acid binding. The phytochemicals consistently form hydrogen bonds with these residues, indicating stable engagement in the ligand-binding domain (Fig. 5F).

4.5. Molecular dynamics simulation indicates stability of compounds' interaction with the protein targets

RMSD backbone provides an overview of the structural stability between the protein and ligand during 20 ns simulations. Most complexes maintained RMSD values below 3 Å, indicating overall stability. Moracin C and D-Glucopyranuronic acid exhibited low RMSD fluctuations when interacting with ESR1 compared to the inhibitor, suggesting stable binding modes. On the other hand, curcumin II with EGFR exhibited larger deviations after 15 ns, implying weaker stabilization compared to the inhibitor. Similarly, curcumin II and MTOR showed higher fluctuations, whereas 5,7,4′-Trihydroxy-6-prenylflavanone closely matched with the inhibitor, indicating a strong interaction.

Hydrogen bond profiles revealed that the bioactive compounds form dynamic but consistent interactions throughout the simulation. Moracin C and 5,7,4′-Trihydroxy-6-prenylflavanone, interacting with ESR1 and PIK3CA, showed comparable or higher hydrogen bonds compared to the inhibitors, highlighting their strong affinity. In contrast, curcumin II, interacting with EGFR and MTOR, exhibited fewer hydrogen bonds, which may contribute to the less stable and significant RMSD fluctuation.

Binding energy analysis showed that most bioactive compounds have comparable or more favorable binding energy than each inhibitor. Moracin C and D-Glucopyranuronic acid, interacting with ESR1, maintained lower binding energy compared to the inhibitors, indicating strong binding stability. In addition, 5,7,4′-Trihydroxy-6-prenylflavanone with PIK3CA exhibited consistent binding energy and stronger binding affinity than the inhibitor. Moreover, curcumin II with EGFR and MTOR relatively have higher binding energy, aligning with low hydrogen bond and RMSD patterns' instability.

Future research is required to perform a study of the most promising compound, particularly 5,7,4-Trihydroxy-6-prenylflavanone, to confirm the bioactivity in relevant breast cancer models. In addition, further synergistic mechanism analysis among components of the formulation would help clarify their therapeutic potential.

5. Conclusions

The study found that polyherbal formulations comprising *Curcuma longa, Phyllanthus niruri, Nigella sativa, Ziziphus mauritiana,* and *Annona muricata* contain various bioactive compounds, such as curcumin, curcumin II, moracin C, 5,7,4′-Trihydroxy-6-prenylflavanone, and D-Glucopyranuronic acid. The compounds showed strong potential as anticancer agents by screening for drug-likeness, membrane permeability, bioactivity, and toxicity. Curcumin II and 5,7,4′-Trihydroxy-6-prenylflavanone interacted with MTOR and PIK3CA, respectively, and then exhibited favorable and comparable binding affinity compared to the inhibitor. The molecular dynamics simulation demonstrates that bioactive compounds targeting ESR1, which are moracin C and D-Glucopyranuronic acid, then PIK3CA, with 5,7,4′-Trihydroxy-6-prenylflavanone, demonstrate minimal RMSD fluctuation, sustained hydrogen bond, and favorable binding energy. EGFR with curcumin exhibits moderate stability. However, this finding still needs to be confirmed using further experimental analysis and integrating data from multi-omics techniques and epigenetic studies. Further QSPR and QSAR modelling could deepen the understanding and identify additional molecular targets involved in breast cancer progression. Compound analysis using chromatography and spectrophotometry is needed to analyze the main compound.

Ethics and Funding

This study did not involve human participants or animals. Therefore, ethical approval was not required. This study was funded by the Ministry of Higher Education, Science, and Technology, Indonesia.

Conflicts of interest

The authors declared no conflict of interest.

Acknowledgments

This research was funded by the Ministry of Higher Education, Science, and Technology of Indonesia in the Program Magister Menuju Doktor untuk Sarjana Unggul (PMDSU) [grant no. 064/C3/DT.05.00/PL/2025].

References

[1] Y. Feng, M. Spezia, S. Huang, C. Yuan, Z. Zeng, L. Zhang, X. Ji, W. Liu, B. Huang, W. Luo, B. Liu, Y. Lei, S. Du, A. Vuppalapati, H.H. Luu, R.C. Haydon, T.-C. He, G. Ren,

Breast cancer development and progression: risk factors, cancer stem cells, signaling pathways, genomics, and molecular pathogenesis, Genes. Dis. 5 (2018) 77–106, https://doi.org/10.1016/j.gendis.2018.05.001.
[2] J. Kim, A. Harper, V. McCormack, H. Sung, N. Houssami, E. Morgan, M. Mutebi, G. Garvey, I. Soerjomataram, M.M. Fidler-Benaoudia, Global patterns and trends in breast cancer incidence and mortality across 185 countries, Nat. Med. 31 (2025) 1154–1162, https://doi.org/10.1038/s41591-025-03502-3.
[3] W. Gautama, Breast cancer in Indonesia in 2022: 30 years of marching in place, Indonesian J. Cancer 16 (2022) 1–2, https://doi.org/10.33371/ijoc.v16i1.920.
[4] C. Tommasi, R. Balsano, M. Corianò, B. Pellegrino, G. Saba, F. Bardanzellu, N. Denaro, M. Ramundo, I. Toma, A. Fusaro, S. Martella, M.M. Aiello, M. Scartozzi, A. Musolino, C. Solinas, Long-term effects of breast cancer therapy and care: calm after the storm? JCM 11 (2022) 1–17, https://doi.org/10.3390/jcm11237239.
[5] S. Sudha, A. Sneha, A. Punitha, S.P. Sargunan, K. Vishwa, Synergistic effect of polyherbal extract containing Indigenous medicinal plants, AJOAIMS 7 (2025) 60–75, https://doi.org/10.56557/ajoaims/2025/v7i1154.
[6] I.O. Lawal, S.O. Olajuyigbe, I.A. Akinwumi, D. Olugbami, Assessment of plants used in polyherbal formulations for traditional treatment of skin infections in ibadan metropolis, J. Herb. Med. 47 (2024) 1–8, https://doi.org/10.1016/j.hermed.2024.100919.
[7] D. Liu, Z. Chen, The effect of curcumin on breast cancer cells, J. Breast Cancer 16 (2013) 133–137, https://doi.org/10.4048/jbc.2013.16.2.133.
[8] S.H. Lee, I.B. Jaganath, N. Atiya, R. Manikam, S.D. Sekaran, Suppression of ERK1/2 and hypoxia pathways by four Phyllanthus species inhibits metastasis of human breast cancer cells, J. Food Drug Anal. 24 (2016) 855–865, https://doi.org/10.1016/j.jfda.2016.03.010.
[9] T. Mishra, M. Khullar, A. Bhatia, Anticancer potential of aqueous ethanol seed extract of *Ziziphus mauritiana* against cancer cell lines and ehrlich ascites carcinoma, Evid. Based Complement. Alternat. Med. 1 (2011) 1–11, https://doi.org/10.1155/2011/765029.
[10] S. Das, A. Ghosh, P. Upadhyay, S. Sarker, M. Bhattacharjee, P. Gupta, S. Chattopadhyay, S. Ghosh, P. Dhar, A. Adhikary, A mechanistic insight into the potential anti-cancerous property of Nigella sativa on breast cancer through microRNA regulation: an in vitro & in vivo study, Fitoterapia 169 (2023) 1–15, https://doi.org/10.1016/j.fitote.2023.105601.
[11] K.K. Silihe, W.D. Mbou, J.C. Ngo Pambe, L.V. Kenmogne, L.F. Maptouom, M.T. Kemegne Sipping, S. Zingue, D. Njamen, Comparative anticancer effects of Annona muricata Linn (Annonaceae) leaves and fruits on DMBA-induced breast cancer in female rats, BMC Complement Med. Ther. 23 (2023) 1–16, https://doi.org/10.1186/s12906-023-04073-x.
[12] P. Wee, Z. Wang, Epidermal growth factor receptor cell proliferation signaling pathways, Cancers (Basel) 9 (2017) 1–45, https://doi.org/10.3390/cancers9050052.
[13] P. Seshacharyulu, M.P. Ponnusamy, D. Haridas, M. Jain, A.K. Ganti, S.K. Batra, Targeting the EGFR signaling pathway in cancer therapy, Expert. Opin. Ther. Targets 16 (2012) 15–31, https://doi.org/10.1517/14728222.2011.648617.
[14] I. Mayer, Role of mTOR inhibition in preventing resistance and restoring sensitivity to hormone-targeted and HER2-Targeted therapies in breast cancer, Clin. Adv. Hematol. Oncol. 11 (2013) 217–224. https://pmc.ncbi.nlm.nih.gov/articles/PMC3774138/.
[15] A.V. González-de-Peredo, A. Maroto, G.F. Barbero, A. Memboeuf, Profiling of organosulfur compounds in onions: a comparative study between LC-HRMS and DTD-GC-MS, Chemosensors 12 (2024) 1–23, https://doi.org/10.3390/chemosensors12070130.
[16] F. Wang, D. Allen, S. Tian, E. Oler, V. Gautam, R. Greiner, T.O. Metz, D.S. Wishart, CFM-ID 4.0 – a web server for accurate MS-based metabolite identification, Nucleic Acids Res. 50 (2022) 165–174, https://doi.org/10.1093/nar/gkac383.
[17] A. Daina, O. Michielin, V. Zoete, SwissADME: a free web tool to evaluate pharmacokinetics, drug-likeness and medicinal chemistry friendliness of small molecules, Sci Rep 7 (2017) 1–13, https://doi.org/10.1038/srep42717.
[18] P. Banerjee, E. Kemmler, M. Dunkel, R. Preissner, ProTox 3.0: a webserver for the prediction of toxicity of chemicals, Nucleic Acids Res. 52 (2024) 513–520, https://doi.org/10.1093/nar/gkae303.
[19] A.M.M. Gomes, P.J. Costa, M. Machuqueiro, Recent advances on molecular dynamics-based techniques to address drug membrane permeability with atomistic detail, BBA Adv. 4 (2023) 1–7, https://doi.org/10.1016/j.bbadva.2023.100099.
[20] A.L. Lomize, J.M. Hage, K. Schnitzer, K. Golobokov, M.B. LaFaive, A.C. Forsyth, I.D. Pogozheva, PerMM: a web tool and database for analysis of passive membrane permeability and translocation pathways of bioactive molecules, J. Chem. Inf. Model. 59 (2019) 3094–3099, https://doi.org/10.1021/acs.jcim.9b00225.
[21] A.A. Lagunin, V.I. Dubovskaja, A.V. Rudik, P.V. Pogodin, D.S. Druzhilovskiy, T.A. Gloriozova, D.A. Filimonov, N.G. Sastry, V.V. Poroikov, CLC-Pred: a freely available web-service for in silico prediction of human cell line cytotoxicity for drug-like compounds, PLoS One 13 (2018) 1–13, https://doi.org/10.1371/journal.pone.0191838.
[22] L. Chen, C. Chu, J. Lu, X. Kong, T. Huang, Y.-D. Cai, Gene ontology and KEGG pathway enrichment analysis of a drug target-based classification system, PLoS One 10 (2015) 1–12, https://doi.org/10.1371/journal.pone.0126492.
[23] M.H. Widyananda, F. Fatchiyah, L. Muflikhah, S.M. Ulfa, N. Widodo, Computational examination to reveal Kaempferol as the most potent active compound from *Euphorbia hirta* against breast cancer by targeting AKT1 and ERα, Egypt. J. Basic Appl. Sci. 10 (2023) 753–767, https://doi.org/10.1080/2314808X.2023.2272385.
[24] Md.M. Rahman, T. Saha, K.J. Islam, R.H. Suman, S. Biswas, E.U. Rahat, Md.R. Hossen, R. Islam, M.N. Hossain, A.A. Mamun, M. Khan, M.A. Ali, M.A. Halim, Virtual screening, molecular dynamics and structure–activity relationship studies to identify potent approved drugs for Covid-19 treatment, J. Biomol. Struct. Dyn. 39 (2021) 6231–6241, https://doi.org/10.1080/07391102.2020.1794974.
[25] P.L. Bremer, A. Vaniya, T. Kind, S. Wang, O. Fiehn, How well can we predict mass spectra from structures? Benchmarking competitive fragmentation modeling for metabolite identification on untrained tandem mass spectra, J. Chem. Inf. Model. 62 (2022) 4049–4056, https://doi.org/10.1021/acs.jcim.2c00936.
[26] R. Magny, Y. Beauxis, G. Genta-Jouve, E. Bourgogne, Application of a molecular networking approach using LC-HRMS combined with the MetWork webserver for clinical and forensic toxicology, Heliyon 10 (2024) e36735, https://doi.org/10.1016/j.heliyon.2024.e36735, 1-11.
[27] M.A. Salem, R.A. El-Shiekh, A.R. Fernie, S. Alseekh, A. Zayed, Metabolomics-based profiling for quality assessment and revealing the impact of drying of Turmeric (*Curcuma longa L.*), Sci. Rep. 12 (2022) 1–11, https://doi.org/10.1038/s41598-022-13882-y.
[28] O.E. Abdel-Sattar, R.M. Allam, A.M. Al-Abd, B. Avula, K. Katragunta, I.A. Khan, A.M. El-Desoky, S.O. Mohamed, A. El-Halawany, E. Abdel-Sattar, M.R. Meselhy, Cytotoxic and chemomodulatory effects of Phyllanthus niruri in MCF-7 and MCF-7ADR breast cancer cells, Sci Rep 13 (2023) 1–16, https://doi.org/10.1038/s41598-023-29566-0.
[29] S. Sun, J. Liu, X. Sun, W. Zhu, F. Yang, L. Felczak, Q. Ping Dou, K. Zhou, Novel annonaceous acetogenins from Graviola (Annona muricata) fruits with strong anti-proliferative activity, Tetrahedron Lett. 58 (2017) 1895–1899, https://doi.org/10.1016/j.tetlet.2017.04.016.
[30] S. Soraya, E. Sukara, E. Sinaga, Identification of chemical compounds in Ziziphus mauritiana fruit juice by GC-MS

and LC-MS/MS analysis, IJBPCS 4 (2022) 11–19, https://doi.org/10.32996/ijbpcs.2022.4.2.2.
[31] C.-Y. Jia, J.-Y. Li, G.-F. Hao, G.-F. Yang, A drug-likeness toolbox facilitates ADMET study in drug discovery, Drug Discov. Today 25 (2020) 248–258, https://doi.org/10.1016/j.drudis.2019.10.014.
[32] D. Klimoszek, M. Jeleń, M. Dołowy, B. Morak-Młodawska, Study of the lipophilicity and ADMET parameters of new anticancer diquinothiazines with pharmacophore substituents, Pharmaceuticals 17 (2024) 1–21, https://doi.org/10.3390/ph17060725.
[33] K. Saritha, M. Alivelu, M. Mohammad, Drug-likeness analysis, in silico ADMET profiling of compounds in Kedrostis foetidissima (Jacq.) Cogn, and antibacterial activity of the plant extract, in: Silico Pharmacol., 12, 2024, pp. 1–11, https://doi.org/10.1007/s40203-024-00240-1.
[34] C.L. Pires, M.J. Moreno, Improving the accuracy of permeability data to gain predictive power: assessing sources of variability in assays using cell monolayers, Membranes 14 (2024) 1–38, https://doi.org/10.3390/membranes14070157.
[35] M. Cai, Y. Xiang, Z. Li, J. Xie, F. Wen, Network pharmacology and molecular docking predictions of the active compounds and mechanism of action of Huangkui capsule for the treatment of idiopathic membranous nephropathy, Medicine 102 (2023) 1–13, https://doi.org/10.1097/MD.0000000000035214.
[36] C. Dhar, Utilizing publicly available cancer clinicogenomic data on CBioPortal to compare epidermal growth factor receptor mutant and wildtype non-small cell lung cancer, Cureus (2021) 1–9, https://doi.org/10.7759/cureus.14683.
[37] A. Asaduzzaman, C.C. Thompson, F.N. Sibai, M.J. Uddin, Using The cancer genome atlas from cBioPortal to develop genomic datasets for machine learning assisted cancer treatment, 2025, pp. 1–22, https://doi.org/10.1101/2025.02.17.638660.
[38] N. Jacobi, R. Seeboeck, E. Hofmann, A. Eger, ErbB family signalling: a paradigm for oncogene addiction and personalized oncology, Cancers 9 (2017) 1–24, https://doi.org/10.3390/cancers9040033.
[39] U.K. Soni, L. Jenny, R.S. Hegde, IGF-1R targeting in cancer – does sub-cellular localization matter? J. Exp. Clin. Cancer Res. 42 (2023) 1–12, https://doi.org/10.1186/s13046-023-02850-7.
[40] A.A. Krygowska, E. Castellano, PI3K: a crucial piece in the RAS signaling puzzle, Cold Spring Harb. Perspect. Med. 8 (2018) 1–19, https://doi.org/10.1101/cshperspect.a031450.
[41] Q. Hu, Q. Bian, D. Rong, L. Wang, J. Song, H.-S. Huang, J. Zeng, J. Mei, P.-Y. Wang, JAK/STAT pathway: extracellular signals, diseases, immunity, and therapeutic regimens, Front. Bioeng. Biotechnol. 11 (2023) 1–24, https://doi.org/10.3389/fbioe.2023.1110765.
[42] Y. Zheng, J. Gierut, Z. Wang, J. Miao, J.M. Asara, A.L. Tyner, Protein tyrosine kinase 6 protects cells from anoikis by directly phosphorylating focal adhesion kinase and activating AKT, Oncogene 32 (2013) 4304–4312, https://doi.org/10.1038/onc.2012.427.
[43] F. Erdogan, T.B. Radu, A. Orlova, A.K. Qadree, E.D. De Araujo, J. Israelian, P. Valent, S.M. Mustjoki, M. Herling, R. Moriggl, P.T. Gunning, JAK-STAT core cancer pathway: an integrative cancer interactome analysis, J. Cell Mol. Med. 26 (2022) 2049–2062, https://doi.org/10.1111/jcmm.17228.
[44] Y.L. Weng, S.R. Naik, N. Dingelstad, M.R. Lugo, S. Kalyaanamoorthy, A. Ganesan, Molecular dynamics and in silico mutagenesis on the reversible inhibitor-bound SARS-CoV-2 main protease complexes reveal the role of lateral pocket in enhancing the ligand affinity, Sci Rep 11 (2021) 1–22, https://doi.org/10.1038/s41598-021-86471-0.
[45] Y. Wang, J. Yu, R. Cui, J. Lin, X. Ding, Curcumin in treating breast cancer: a review, J. Lab. Autom. 21 (2016) 723–731, https://doi.org/10.1177/2211068216655524.
[46] S.M.W. Kusuma, D.H. Utomo, R. Susanti, Molecular mechanism of inhibition of cell proliferation: an in silico study of the active compounds in *Curcuma longa* as an anticancer, J. Tropical Biodiv. Biotechnol. 7 (2022) 1–16, https://doi.org/10.22146/jtbb.74905.
[47] S. Sun, M. Zhang, M. Li, F. Guan, F. Wu, X. Feng, B. Xia, H. Zhang, Compounds inhibiting hyperglycemia and cancer cell proliferation from Morus alba L, Planta Med. 78 (2012) 1–10, https://doi.org/10.1055/s-0032-1320944.
[48] X. Yao, D. Wu, N. Dong, P. Ouyang, J. Pu, Q. Hu, J. Wang, W. Lu, J. Huang, C. Moracin, A phenolic compound isolated from Artocarpus heterophyllus, suppresses lipopolysaccharide-activated inflammatory responses in Murine Raw264.7 macrophages, Int. J. Math. Stat. 17 (2016) 1–15, https://doi.org/10.3390/ijms17081199.
[49] A. Sychrová, G. Škovranová, M. Čulenová, S.B. Fialová, Prenylated flavonoids in topical infections and wound healing, Molecules 27 (2022) 1–49, https://doi.org/10.3390/molecules27144491.
[50] O. Ursu, A. Rayan, A. Goldblum, T.I. Oprea, Understanding drug-likeness, WIREs Comput. Mol. Sci. 1 (2011) 760–781, https://doi.org/10.1002/wcms.52.
[51] B.J. Bennion, N.A. Be, M.W. McNerney, V. Lao, E.M. Carlson, C.A. Valdez, M.A. Malfatti, H.A. Enright, T.H. Nguyen, F.C. Lightstone, T.S. Carpenter, Predicting a drug's membrane permeability: a computational model validated with *in vitro* permeability assay data, J. Phys. Chem. B 121 (2017) 5228–5237, https://doi.org/10.1021/acs.jpcb.7b02914.
[52] P. Jamkhande, M. Ghante, R. Kshirsaga, In silico PASS predictions and exploration of antioxidant and anti-inflammatory activity of citrus karna raf, Fruit MMJ (2024) 49–58, https://doi.org/10.4274/MMJ.galenos.2024.49775.
[53] M. Giorgini, M. Taroncher, M.-J. Ruiz, Y. Rodríguez-Carrasco, J. Tolosa, In vitro and predictive computational toxicology methods for the neurotoxic pesticide amitraz and its metabolites, Brain Sci. 13 (2023) 1–17, https://doi.org/10.3390/brainsci13020252.
[54] S. Sigismund, D. Avanzato, L. Lanzetti, Emerging functions of the EGFR in cancer, Mol. Oncol. 12 (2018) 3–20, https://doi.org/10.1002/1878-0261.12155.
[55] J.L. Hsu, M.-C. Hung, The role of HER2, EGFR, and other receptor tyrosine kinases in breast cancer, Cancer Metastasis Rev. 35 (2016) 575–588, https://doi.org/10.1007/s10555-016-9649-6.
[56] K. Ganesan, C. Xu, S. Wu, Y. Sui, B. Du, J. Zhang, F. Gao, J. Chen, H. Tang, Ononin inhibits tumor bone metastasis and osteoclastogenesis by targeting mitogen-activated protein kinase pathway in breast cancer, Research 7 (2024) 1–17, https://doi.org/10.34133/research.0553.
[57] S. Baldi, N. Long, S. Ma, L. Liu, A. Al-Danakh, Q. Yang, X. Deng, J. Xie, H. Tang, Advancements in protein kinase inhibitors: from discovery to clinical applications, Research 8 (2025) 1–29, https://doi.org/10.34133/research.0747.
[58] D. Yu, M.-C. Hung, Role of erbB2 in breast cancer chemosensitivity, Bioessays 22 (2000) 673–680, https://doi.org/10.1002/1521-1878(200007)22:7<673::AID-BIES10>3.0.CO;2-A.
[59] T. Murai, Transmembrane signaling through single-spanning receptors modulated by phase separation at the cell surface, Eur. J. Cell. Biol. 103 (2024) 1–9, https://doi.org/10.1016/j.ejcb.2024.151413.
[60] A. Alwhaibi, A. Verma, M.S. Adil, P.R. Somanath, The unconventional role of Akt1 in the advanced cancers and in diabetes-promoted carcinogenesis, Pharmacol. Res. 145 (2019) 1–21, https://doi.org/10.1016/j.phrs.2019.104270.
[61] E. Paplomata, R. O'Regan, The PI3K/AKT/mTOR pathway in breast cancer: targets, trials and biomarkers, The.r Adv. Med. Oncol. 6 (2014) 154–166, https://doi.org/10.1177/1758834014530023.
[62] S. Yang, C. Manna, P.R. Manna, Harnessing the role of ESR1 in breast cancer: correlation with microRNA, lncRNA, and methylation, Int. J. Math. Stat. 26 (2025) 1–17, https://doi.org/10.3390/ijms26073101.